

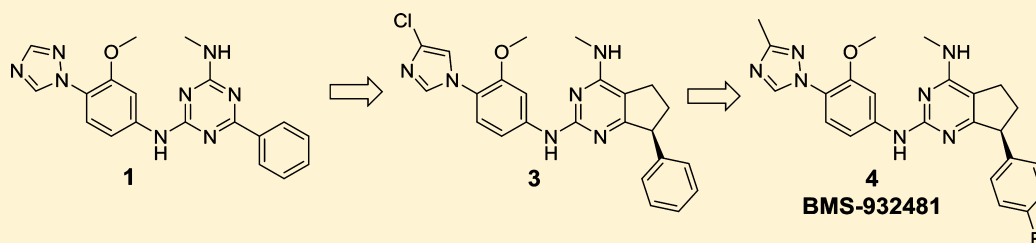
Identification and Preclinical Evaluation of the Bicyclic Pyrimidine γ -Secretase Modulator BMS-932481

Kenneth M. Boy,^{*,†,◆} Jason M. Guernon,^{†,||} Dmitry S. Zuev,^{†,⊥} Li Xu,^{†,§} Yunhui Zhang,^{†,||} Jianliang Shi,^{†,||} Lawrence R. Marcin,^{†,●} Mendi A. Higgins,^{†,§} Yong-Jin Wu,^{†,◆} Subramaniam Krishnananthan,^{†,||} Jianqing Li,^{†,◆} Ashok Trehan,[†] Daniel Smith,^{†,||} Jeremy H. Toyn,^{†,||} Jere E. Meredith,^{†,○} Catherine R. Burton,[†] S. Roy Kimura,^{†,■} Tatyana Zvyaga,^{†,§} Xiaoliang Zhuo,^{†,◆} Kimberley A. Lentz,^{†,△} James E. Grace,^{†,◇} Rex Denton,^{†,||} John S. Morrison,^{†,||} Arvind Mathur,[‡] Charles F. Albright,^{†,●} Michael K. Ahljianian,^{†,◇} Richard E. Olson,^{†,◆} Lorin A. Thompson,^{†,□} and John E. Macor^{†,▽}

[†]Bristol-Myers Squibb, Wallingford, Connecticut 06492, United States

[‡]Bristol-Myers Squibb, Princeton, New Jersey 08543, United States

Supporting Information



ABSTRACT: A triazine hit identified from a screen of the BMS compound collection was optimized for potency, in vivo activity, and off-target profile to produce the bicyclic pyrimidine γ -secretase modulator BMS-932481. The compound showed robust reductions of $A\beta_{1-42}$ and $A\beta_{1-40}$ in the plasma, brain, and cerebrospinal fluid of mice and rats. Consistent with the γ -secretase modulator mechanism, increases in $A\beta_{1-37}$ and $A\beta_{1-38}$ were observed, with no change in the total amount of $A\beta_{1-x}$ produced. No Notch-based toxicity was observed, and the overall preclinical profile of BMS-932481 supported its further evaluation in human clinical trials.

KEYWORDS: Alzheimer's disease, clinical candidate, gamma-secretase modulator, bicyclic pyrimidine

Alzheimer's disease (AD) is a neurodegenerative disorder of the elderly. Progressively worsening symptoms include memory loss, difficulty with language and abstract thinking, difficulty with familiar tasks, and impaired recognition of family and friends. Death occurs on average 10 years after initial diagnosis. The prevalence of AD in the U.S. is ca. 5.7 million people and is expected to grow significantly in the coming decades.¹ The pathology of AD precedes the onset of symptoms by a decade or more and is characterized by the deposition of amyloid plaques and neurofibrillary tangles in the brain. The current standard of care, acetylcholinesterase inhibitors and an NMDA antagonist, provides minimal and temporary benefit, and does not prevent progression of the disease. Much of AD drug discovery has focused on reducing the production of the $A\beta$ peptides, which produce the characteristic amyloid plaques found in the brain. Inhibitors of the enzymes responsible for $A\beta$ production, beta- and gamma-secretase (GS), have entered clinical trials but have failed to achieve commercialization. Recently, several late-stage trials of beta-secretase (BACE) inhibitors failed to achieve clinical success. Merck has announced that the study of

verubecestat in prodromal AD patients was suspended following an interim safety analysis that predicted an inadequate benefit/risk ratio,² and AstraZeneca/Lilly has terminated the study of lanabecestat in AD patients with either mild cognitive impairment or mild dementia³ because it was unlikely to meet the primary end points of the trial.⁴ Likewise, despite the enormous effort expended to advance six different gamma-secretase inhibitors (GSIs) into Phase II/III clinical trials, these agents failed in part due to toxicity stemming from suppressing the proteolysis of other GS substrates, most notably Notch.⁵ An alternative drug mechanism, gamma-secretase modulators (GSMs), seeks to exploit the differing potential of the several endogenous $A\beta_{1-x}$ peptide species to aggregate to form neurotoxic oligomers. Specifically, GSMs shift the distribution of gamma secretase cleavage products away from the longer $A\beta_{1-42}$ and $A\beta_{1-40}$

Received: November 9, 2018

Accepted: February 4, 2019

Published: February 17, 2019

peptides to the shorter forms $A\beta_{1-38}$ and $A\beta_{1-37}$.⁶ The shorter species are less lipophilic, less aggregation-prone, and less neurotoxic than aggregates of $A\beta_{1-42}$ and, in fact, may play a direct role in hindering the aggregation of $A\beta_{1-42}$.⁷ Importantly, toxicity arising from the suppression of the Notch signaling pathway is avoided by the GSM mechanism because GS activity is not inhibited. Thus, GSMs offer an attractive alternative disease-modifying mechanism to avoid GSI toxicity.

Efforts in our laboratories to discover a GSM began with a screen⁸ of the BMS compound collection, which identified triazine **1** (Figure 1). The IC_{50} for $A\beta_{1-42}$ lowering was 120

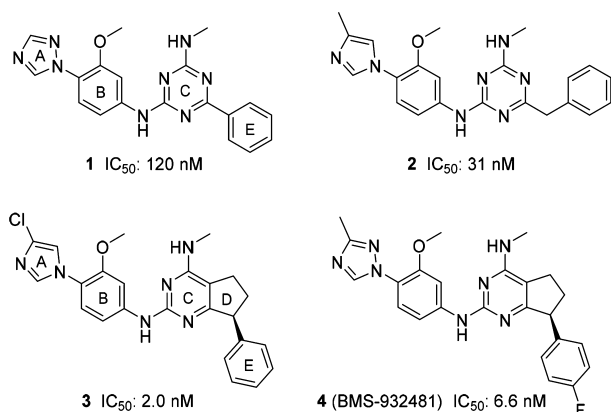


Figure 1. Novel triazine/pyrimidine γ -secretase modulators.

nM in our primary H4 cell-based assay.⁹ No effect was seen on total $A\beta_{1-x}$ formation, whereas increased levels of $A\beta_{1-37}$ and $A\beta_{1-38}$ were observed in experiments using urea gel Western blotting (data not shown). Taken together, these results firmly establish **1** as a GSM. The central triazine core (C ring, Figure 1), flanked by a triazolyl anisole biaryl moiety (A–B rings) and an aromatic group (E ring), was topologically similar to other GSMs known in the patent literature. However, both the Eisai cinnamide¹⁰ and Schering–Plough alkenyl oxadiazole¹¹ chemotypes possessed a methine linker between the B- and C-rings, so the aniline NH linking the B and C rings in **1** was unique in the public literature at that time.¹² Additionally, the triazine 4-NHMe substituent represented an additional vector for potential optimization.

Compound **1** was rapidly modified to incorporate a 4-methylimidazole A-ring and benzyl E-ring to form compound **2**, which was potent ($A\beta_{1-42}$ IC_{50} = 31 nM) in our primary assay. Triple transgenic LaFerla mice,¹³ which exhibit accelerated plaque and tangle pathology resulting from the presence of the APP Swedish, MAPT P301L, and PSEN1M146V mutations, were orally dosed at 30 mg/kg with compound **2** in a solution formulation. At 3 h postdose, a 32% reduction in brain $A\beta_{1-42}$ was observed, with a brain to plasma concentration ratio (B/P) = 0.47. Compound **2** exhibited liabilities that would need to be addressed in subsequent compounds, specifically a short half-life as a consequence of ubiquitous metabolism, potent hERG inhibition, and potent and time-dependent CYP3A4 inhibition. After extensive structure–activity relationship exploration, we identified and integrated two structural modifications leading to pyrimidine **3**. First, the change from a triazine to a pyrimidine C-ring core permitted the fusion of an additional carbocyclic ring (D-ring, Figure 1), which restricted the

position of the aryl E-ring relative to the core. Second, replacement of the 4-methylimidazole A-ring with 4-chloroimidazole provided an improvement in both potency and CYP3A4 inhibition profile. Together, these features increased the potency of **3** vs **2** by an order of magnitude (IC_{50} = 2.0 nM). Consistent with its high potency relative to **2**, compound **3** demonstrated an in vivo pharmacologic response in multiple species. In LaFerla mice, a 30 mg/kg oral dose of **3** reduced the level of brain $A\beta_{1-42}$ by 86% after 3 h, and in Harlan Sprague–Dawley rats, a 10 mg/kg oral dose reduced $A\beta_{1-42}$ by 59% 3 h postdose. The corresponding plasma concentrations were 2.1 μ M in LaFerla mice and 1.7 μ M in rat, and the B/P ratio in rats was 0.38. Furthermore, the metabolic profile of **3** was improved over **2**, with 96% of parent compound remaining after a 10 min incubation with human liver microsomes,¹⁴ while in vitro biotransformation assays showed that metabolism was confined to N-demethylation and monohydroxylation of the D-ring. An AUC_{0-24h} of 7.6 μ M·h elicited our targeted 25% AUC_{0-24h} reduction¹⁵ of rat brain $A\beta_{1-42}$. Allometric scaling of the results from similar experiments in dog and cynomolgus monkey predicted a human dose for 25% lowering of $A\beta_{1-42}$ of 90 mg QD (1.3 mg/kg), aided by the oral bioavailability across species (49%, 64%, and 44% in rat, dog, and cynomolgus monkey, respectively).

Given the improvements in PK/PD relative to **2**, we profiled **3** for safety. Patch-clamp electrophysiology revealed potent inhibition of the hERG ion channel (IC_{50} = 200 nM). However, the low free fraction of **3** (0.1%) contributed to a satisfactory predicted safety margin with regard to hERG-mediated cardiac events since the QRT elongation effects of hERG inhibition are driven by the free-drug concentration. This prediction was confirmed by a rabbit telemetry study, which demonstrated a 40-fold safety margin vs the hERG NOAEL of 15 μ M. Compound **3** was then tested in rats for 4 days after oral dosing at 10, 30, and 100 mg/kg. Visibly yellow plasma at all doses alerted us to an increase in unconjugated bilirubin, and upon further investigation, significant inhibition of hUGT1A1 (IC_{50} = 1.4 μ M) and OATP1B1 (690 nM) was found. Furthermore, detailed tissue examination from the same study also revealed hepatocellular necrosis at all doses studied, which precluded a viable path forward for this compound.

It is widely recognized that high lipophilicity is associated with a greater chance of drug toxicity,¹⁶ and in light of the profile of **3**, we pursued a strategy of lowering cLogP. Reducing lipophilicity in CNS drugs can be particularly challenging since overly polar molecules generally fail to cross the blood–brain barrier, and many CNS targets often prefer lipophilic compounds.¹⁷ Thus, balancing potency and polarity for CNS drugs in general, and GSMs in particular, is a well-recognized challenge.¹⁸ After examining compounds from several sub-series, we found that (S)-7-(4-fluorophenyl)-N²-(3-methoxy-4-(3-methyl-1H-1,2,4-triazol-1-yl)phenyl)-N⁴-methyl-6,7-dihydro-5H-cyclopenta[d]pyrimidine-2,4-diamine (**4**, BMS-932481) had the best balance of potency, efficacy, and off-target profile (Table 1).

Compound **4** differs from compound **3** primarily by changing the A-ring to the more polar 3-methyl triazole, which resulted in an increased free fraction (0.6%), consistent with our strategy. The $A\beta_{1-42}$ IC_{50} of **4** was 6.6 nM, slightly less potent than **3**, highlighting a trade-off between potency and polarity. Importantly, and consistent with the GSM mechanism, treatment of cultured H4-APPsw cells with **4**

Table 1. Key Parameters of Compounds 2, 3, and 4

	2	3	4
IC ₅₀ Aβ ₁₋₄₂ (nM) ^a	31	2.0	6.6
Aβ ₁₋₄₂ reduction in mice ^b (%)	32	86	81
Aβ ₁₋₄₂ reduction in rats ^c (%)		59	41
shake flask log D (pH 6.5)		4.42	3.97
human plasma free fraction		0.1	0.6
active AUC ₀₋₂₄ (μM·h)		7.6	4.0
calcd human efficacious dose (mg QD)		90	110

^a*n* = 315, 68, and 12, respectively. ^bReduction in brain Aβ₁₋₄₂, LaFerla mice, 30 mg/kg po, 3 h postdose, *n* = 3. ^cReduction in brain Aβ₁₋₄₂, Sprague–Dawley rat, 10 mg/kg po, 3 h postdose, *n* = 5.

resulted in a large decrease in Aβ₁₋₄₂ and Aβ₁₋₄₀ and a corresponding increase in Aβ₁₋₃₇ and Aβ₁₋₃₈ (Figure 2) as measured by mass spectrometry. Total Aβ_{1-x} was unchanged at concentrations of 4 up to 10 μM, as determined by Aβ_{1-x} ELISA. Furthermore, the same distribution among Aβ peptide species was recapitulated in both rat brain and CSF after intravenous administration of 4.¹⁹ The amount of Aβ₁₋₄₂ in the brains of wild-type mice was reduced by 81% 3 h after a 30 mg/kg oral dose. In rats dosed orally at 10 mg/kg, brain Aβ₁₋₄₂ was reduced by 41% vs predose levels at the 5 h time point, with a concentration of 1.4 μM in plasma and a B/P ratio of 0.23. Compound 4 showed low clearance in rat (11.2 mL/min/kg), with a volume of distribution of 2.3 L/kg and a half-life of 2.7 h (Table 2). In preclinical species, oral bioavailability was 98%, 85%, and 45% in rat, dog, and cynomolgus monkey, respectively, when dosed as a nanosuspension.²⁰ Further testing in rats enabled generation of a PK/PD relationship fitted to an indirect response model.²¹ When integrating over a 24 h time period, a 3 mg/kg dose reduced brain Aβ₁₋₄₂ AUC by 45% with an exposure of 9.7 μM·h, and a 10 mg/kg dose reduced brain Aβ₁₋₄₂ AUC by 66% with an exposure of 32 μM·h. Using these data, we calculated that a plasma exposure of 4.0 μM·h would achieve a 25% AUC reduction of Aβ₁₋₄₂. Human PK was predicted by allometric scaling of PK results from rat, dog, and cynomolgus monkey. Combining the predicted human PK with the rat PK/PD forecasted that a total oral daily human dose of 110 mg (1.6 mg/kg) would result in a 31% reduction in brain Aβ₁₋₄₂ and that a 446 mg total daily dose would result in a 57% reduction in brain Aβ₁₋₄₂. We observed a low peak-to-trough exposure profile, resulting in a predicted C_{max} at the two doses of 0.32 and 1.3 μM, respectively. The projected human exposure calculations enabled interpretation of the metabolic profiling data.

Compound 4 inhibited recombinant CYP3A4 with an IC₅₀ of 0.51 μM after a 30 min incubation. A more comprehensive assay²² was performed to assess the potential for time-dependent inhibition of CYP3A4. The large K_i of 82.5 μM mitigated the impact of a robust K_{inact} of 0.47 min⁻¹, with the result indicating mild drug–drug interaction potential²³ due to CYP3A4 inhibition at the 110 mg (C_{max} = 0.32 μM, 1000λ = 1.8 min⁻¹) and the 446 mg (C_{max} = 1.3 μM, 1000λ = 7.5 min⁻¹) doses. In human liver microsomes, the compound inhibited the activity of the CYP2C subfamily with single digit micromolar IC₅₀s, and IC₅₀s against the rest of the CYP isoforms tested were greater than 17 μM. PXR in vitro transactivation by compound 4 was evaluated to assess the potential for induction of CYP3A4-mediated metabolism, and 4 was found to have an EC₅₀ of >2.7 μM, with an average Y_{max} of 36% (10 μM rifampicin = 100%). Following up on this

Table 2. Detailed Profile for Compound 4 (BMS-932481)

assay	result		
Aβ ₁₋₄₂ IC ₅₀ (nM); <i>n</i> = 12	6.6 ± 2.3		
Aβ ₁₋₄₀ IC ₅₀ (nM); <i>n</i> = 3	25 ± 8		
Aβ _{x-42} IC ₅₀ (nM); <i>n</i> ≥ 3	5.5 ± 3.6		
total Aβ _{1-x} inhib. at 50 μM (%); <i>n</i> ≥ 3	30 ± 10		
AMES result	negative		
metabolic stability T _{1/2} : human, rat, mouse, cynomolgus monkey, dog (min)	30, 28, 36, 11, 27		
plasma free fraction: human, rat, mouse, cynomolgus monkey, dog (%)	0.6, 0.7, 0.7, 1.3, 0.8		
CYP 450 HLM inhibition IC ₅₀ (μM) 1A2, 2B6, 2C8, 2C9, 2C19, 2D6, 3A4	>40, > 40, 4.5, 7.4, 8.3, 18, 0.2		
CYP 3A4 HLM time-dependent inhib.			
K _i (μM)	83		
K _{inact} (min ⁻¹)	0.47		
hERG IC ₅₀ (μM)	1.2		
Caco-2 P _{app} efflux ratio	3.5, 0.8		
PSA (Å ²)	90		
pK _a , spectrophotometric	2.0, 5.9		
shake flask log D at pH 6.5, 7.4 ^a	3.97, 4.34		
melting point (°C)	230		
aq. solubility ^b at pH 1.0, 6.5 (μg/mL)	19, 0.1		
iv PK parameters	species ^c		
	rat ^d	monkey ^e	dog ^f
t _{1/2} (h)	2.7 ± 0.6	2.9 ± 1.0	8.7 ± 1.1
CL (mL/min/kg)	11.2 ± 0.4	31.3 ± 9.5	12.5 ± 1.2
V _{ss} (L/kg)	2.3 ± 0.4	5.4 ± 0.8	6.1 ± 0.3
F (%) ^f	98	45	85
projected human PK parameters ^g			
dose (mg QD)	110, 446		
C _{max} (μM)	0.32, 1.30		
AUC (μM·h)	4.0, 16.2		
Aβ ₁₋₄₂ reduction (%)	31, 57		

^aOctanol/water partitioning. ^bCrystalline material. ^cSprague–Dawley rat, male cynomolgus monkey, male Beagle dog, pretreated with pentagastrin. ^d2 mg/kg, 5 min iv infusion, 9:1 PEG:EtOH, *n* = 5. ^e1 mg/kg, 5 min iv infusion, 9:1 PEG:EtOH, *n* = 3. ^fDosed as a nanosuspension. ^gAt steady state.

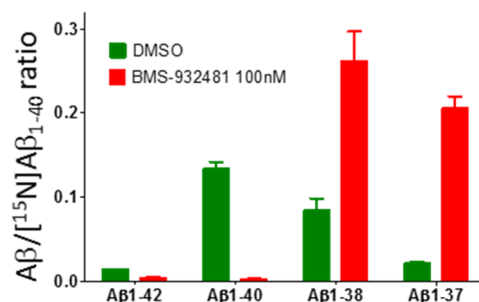


Figure 2. Effect of 4 on Aβ species in cultured H4-APPsw cells. See ref 8, Figure 3 for the general method, and ref 16, Figure 1 for additional data.

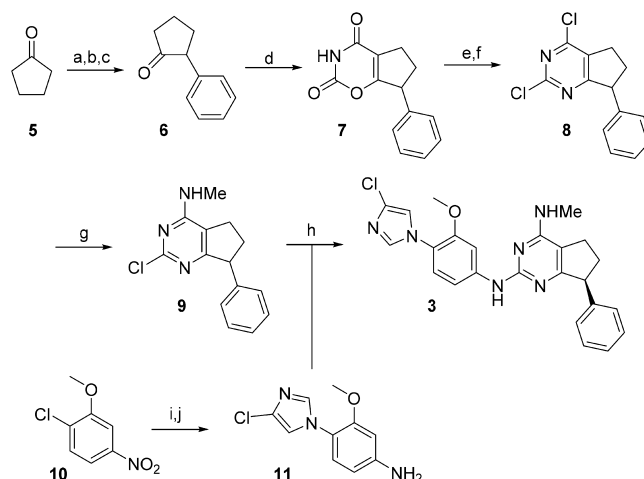
result, CYP3A4 mRNA induction was assessed in cryopreserved primary human hepatocytes. A low (16%) elevation of CYP3A4 mRNA was observed at 1 μM, a concentration approximating the projected C_{max} of 4, whereas a moderate (36–43%) elevation was observed at supra-physiological concentrations (3.3–10 μM). Taken together, these results supported further safety profiling.

Cardiac safety was evaluated in multiple experiments. Compound 4 was 6-fold less potent at hERG than compound 3, a result we interpret as a consequence of its reduced lipophilicity.²⁴ Telemetry data from unconscious rabbits showed no change in QTcf and a 4 ms increase in QTcv after a 3 mg/kg dose (16 μ M exposure). Dosing at 10 mg/kg (50 μ M exposure) resulted in a 3 and 10 ms increase in QTcf and QTcv, respectively. The exposure multiples over the projected clinical C_{\max} were from 50- to 170-fold, consistent with a minimal risk of hERG liability. During these experiments, increased blood pressure and decreased heart rate were observed at doses of 10 mg/kg and higher; however, these effects were not seen in parallel experiments in *conscious* rats at any dose studied. The hemodynamic effects were attributed to the anesthesia used during the rabbit experiments.

Compound 4 was well tolerated in a 2-week oral repeat dose toxicity study in rats at 10, 30, and 100 mg/kg. A minimal, nontoxicologically significant bilirubin elevation was observed, in-line with previous observations in mice and in contrast to the results seen for 3. Subsequent *in vitro* profiling of bilirubin transporter inhibition revealed, surprisingly, that compound 4 had an identical potency at UGT1A1 (1.4 μ M) to compound 3. Additionally, compound 4 potently inhibited the organic anion transporting polypeptide 1B1 (IC_{50} = 66 nM). The lack of correlation between the potency at these transporters and the differential *in vivo* bilirubin levels observed in 3 and 4 is not currently understood; the hepatocellular necrosis uniquely observed with compound 3 may confound a simple interpretation. Findings from the two-week toxicity study were limited to stress and reduced food consumption effects for the high (100 mg/kg) oral dose group, with no Notch-related goblet cell metaplasia in the duodenum, consistent with the gamma-secretase modulator mechanism of action. Additionally, no hepatotoxicity or necrosis was observed. Compound 4 showed a 48-fold margin over the projected human efficacious exposure of 4 μ M·h at the NOAEL of 30 mg/kg. Additionally, an acute oral dose of 300 mg/kg in dogs was tolerated with no significant changes in bilirubin levels or other clinical pathological assessments. The observed C_{\max} and AUC in this experiment were 14 μ M and 180 μ M·h, respectively, translating to a 43-fold margin in C_{\max} and 46-fold in AUC to the projected efficacious clinical dose. Furthermore, in a one-month toxicity study in dogs, the high dose group showed a NOAEL to minimally significant hyperbilirubinemia at 150 mg/kg (40 μ M·h exposure). In total, the toxicity profile supported the progression of compound 4 in human clinical trials.

Compound 3 was synthesized as shown in Scheme 1, starting with Grignard addition of phenylmagnesium bromide to cyclopentanone, followed by dehydration and oxidation to afford 2-phenyl cyclopentanone. Condensation with *N*-(chlorocarbonyl) isocyanate (CCI)²⁵ afforded compound 7 in low yield. Subsequent condensation with ammonia yielded the pyrimidine dione, which was then reacted with phosphoryl chloride to give dichloropyrimidine 8. Reaction with methylamine in THF gave a ~4:1 ratio of monoaddition products favoring the desired 4-aminomethyl regioisomer 9. Aniline 11, derived from the substituted chloro-nitrobenzene 10 by nucleophilic aromatic substitution with chloroimidazole and subsequent reduction of the nitro group, was combined with 9 under acidic conditions to yield compound 3 after resolution by chiral HPLC.

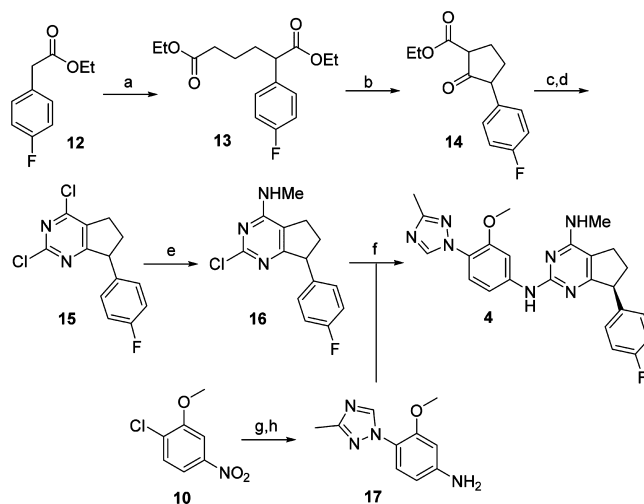
Scheme 1. Initial Synthesis of Compound 3^a



^aReagents and conditions: (a) PhMgBr, THF, 0 °C to rt, 30 min, then reflux, 2 h; (b) 6 N HCl, 100%; (c) 1:4 30% H₂O₂/HCO₂H, 40 °C, 15 min, then add 1-phenylcyclopentene, rt, 4 h [**Caution!**: initial exotherm], 84%; (d) *N*-(chlorocarbonyl)isocyanate, 58 °C, 1 h, then 130 °C, 45 min, 13%; (e) conc. NH₃, 100 °C in sealed tube, 5 h, 100%; (f) POCl₃, 110 °C, microwave, 1 h, 72%; (g) MeNH₂, THF, rt, 69%; (h) 1:1 THF/HOAc, 75 °C, 47%, then separate enantiomers; (i) 4-chloro-1H-imidazole, KOH, DMSO, 80 °C, 20 h, 42%; (j) Fe, 1:2 HOAc/EtOH, 100 °C, 30 min, 97%.

As the program progressed, a more concise synthesis of the key pyrimidine dichloride was developed and used for the preparation of compound 4, as outlined in Scheme 2. Alkylation of ethyl *p*-fluorophenyl acetate 12 with ethyl-4-bromobutanoate afforded diester 13, which then formed the substituted cyclopentanone 14 via Dieckmann condensation. Reaction with molten urea directly provided the pyrimidine dione, which was taken forward in the previously described

Scheme 2. Medicinal Chemistry Synthesis of Compound 4^a



^aReagents and conditions: (a) ethyl-4-bromobutanoate, DMF, Cs₂CO₃, 60 °C, 72 h, 37%; (b) NaHMDS, THF, 0 °C to rt, 2 h, 94%; (c) urea, 150 °C, then add ketoester, 16 h, 35%; (d) POCl₃, *N,N*-diethylaniline, 103 °C, 4 h, 77%; (e) MeNH₂, THF, 2 h, 84%; (f) H₂SO₄, NMP, 100 °C, 18 h, 66%, then separate enantiomers; (g) 3-methyl-1H-1,2,4-triazole, KOH, DMSO, 80 °C, 6 h, 26%; (h) H₂, Pd/C, MeOH, 94%.

manner to penultimate **16**. This route avoided the use of CCl₄, which was both toxic and of limited commercial supply. The yield of the final coupling with aniline **17** was improved by using catalytic sulfuric acid in NMP, which afforded the desired compound **4** after chiral chromatography. The absolute configuration of **4**, as its HCl salt, was proven by X-ray diffraction.²⁶

The results from the phase 1 clinical trial of BMS-932481 have been reported.²⁷ Analysis of both plasma and CSF samples demonstrated a dose-dependent increase in A β _{1–37} and A β _{1–38}, a decrease in A β _{1–42} and A β _{1–40}, and no change in total A β _{1–x} after single oral doses of 10 to 1200 mg, and upon multiweek daily dosing at 50 to 200 mg. BMS-932481 was well tolerated when dosed acutely. ALT elevations were observed after administration of 200 mg of BMT-932481 for 24 days, which was hypothesized to be due to unexpected bioaccumulation of the drug in the liver. Modeling the multiple ascending dose data revealed that a ~25% lowering of A β _{1–42} would be achieved at an exposure deemed free of ALT elevation; however, the decision was made to discontinue the development of BMS-932481 due to the inability to safely escalate the dose to achieve greater A β reduction.

To summarize, we have discovered a bicyclic pyrimidine capable of modulating the activity of gamma-secretase to affect reduction in A β _{1–42} and elevation of shorter A β peptides as a potential treatment for Alzheimer's disease. The acceptable projected human dose and attractive preclinical safety profile supported our decision to evaluate the clinical effect of a low A β _{1–42}/A β _{1–37/38} ratio in human subjects. A more detailed accounting of the broader medicinal chemistry efforts leading to the discovery of BMS-932481 will be reported in due course.

■ ASSOCIATED CONTENT

Supporting Information

The Supporting Information is available free of charge on the ACS Publications website at DOI: 10.1021/acsmchemlett.8b00541.

Synthetic procedures and analytical data for **1–4**, **6–9**, **11**, and **13–17**²⁸ (PDF)

■ AUTHOR INFORMATION

Corresponding Author

*Phone: 617-494-7270. E-mail: Kenneth.Boy@bms.com.

ORCID

Kenneth M. Boy: 0000-0003-3188-8252

Lawrence R. Marcini: 0000-0003-0375-6252

Yong-Jin Wu: 0000-0002-3452-6292

Jianqing Li: 0000-0002-8445-9796

Present Addresses

◆ Bristol-Myers Squibb, Cambridge, MA 02142.

‡ Bristol-Myers Squibb, Princeton, NJ 08543.

§ Bristol-Myers Squibb, Princeton, NJ 08540.

⊥ Cantor Colburn, Hartford, CT 06103.

● Forma Therapeutics, Branford, CT 06405.

¶ Yale University, New Haven, CT 06520.

○ Amgen, Cambridge, MA 02142.

■ Modulus Discovery, Inc., Tokyo, Japan.

△ Bristol-Myers Squibb, Pennington, NJ 06534.

○ Arvinas, New Haven, CT 06511.

● Editas Medicine, Cambridge, MA 02141.

◇ Ani Consulting, LLC, Madison, CT 06443.

□ Fulcrum Therapeutics, Cambridge, MA 02139.

▼ Sanofi, Waltham, MA 02451.

Author Contributions

All authors have given approval to the final version of the manuscript.

Funding

Funding was provided by Bristol-Myers Squibb, who employed all authors at the time this research was conducted.

Notes

The authors declare no competing financial interest.

■ ACKNOWLEDGMENTS

We acknowledge the scientists at the Biocon Bristol-Myers Squibb Research Center (BBRC) for the synthesis of key chemical intermediates, Valerie Guss and Alan Lin for conducting in vivo studies, and Edward Kozlowski for performing chiral separations.

■ ABBREVIATIONS

GS, gamma-secretase; BACE, beta-site APP-cleaving enzyme; GSIs, gamma-secretase inhibitors; GSMs, gamma-secretase modulators; hERG, human ether-a-go-go-related gene; hUGT1A1, human uridine diphosphate glucuronosyltransferase 1A1; OATP1B1, organic ion transporting polypeptide; APP, amyloid precursor protein; MAPT, microtubule-associated protein tau; PSEN, presenilin; PXR, pregnane X receptor; ALT, alanine transaminases

■ REFERENCES

- (1) Alzheimer's Association. 2017 Alzheimer's disease facts and figures. *Alzheimer's Dementia* **2018**, *14*, 367–429.
- (2) Merck press release, February 13, 2018. <http://investors.merck.com/news/press-release-details/2018/Merck-Announces-Discontinuation-of-APECS-Study-Evaluating-Verubecestat-MK-8931-for-the-Treatment-of-People-with-Prodromal-Alzheimers-Disease/default.aspx>, (accessed August 1, 2018).
- (3) Vassar, R. BACE1 inhibitor drugs in clinical trials for Alzheimer's disease. *Alzheimer's Res. Ther.* **2014**, *6*, 89.
- (4) Lilly/Astra-Zeneca press release, June 12, 2018. <https://www.astrazeneca.com/media-centre/press-releases/2018/update-on-phase-iii-clinical-trials-of-lanabecestat-for-alzheimers-disease-12062018.html>, (accessed August 1, 2018).
- (5) Haapasalo, A.; Kovacs, D. M. The many substrates of presenilin/ γ -secretase. *J. Alzheimer's Dis.* **2011**, *25*, 3–28.
- (6) Bulic, B.; Ness, J.; Hahn, S.; Rennhack, A.; Jumpertz, T.; Weggen, S. Chemical biology, molecular mechanism and clinical perspective of γ -secretase modulators in Alzheimer's disease. *Current Neuropharmacology* **2011**, *9*, 598–622.
- (7) Tate, B.; McKee, T. D.; Loureiro, R. M. B.; Dumin, J. A.; Xia, W.; Pojasek, K.; Austin, W. F.; Fuller, N. O.; Hubbs, J. L.; Shen, R.; Jonker, J.; Ives, J.; Bronk, B. S. Modulation of gamma-secretase for the treatment of Alzheimer's disease. *Int. J. Alzheimer's Dis.* **2012**, *2012*, 1.
- (8) Toyn, J. H.; Thompson, L. A.; Lentz, K. A.; Meredith, J. E.; Burton, C. R.; Sankaranarayanan, S.; Guss, V.; Hall, T.; Iben, L. G.; Krause, C. M.; Krause, R.; Lin, X.-A.; Pierdomenico, M.; Polson, C.; Robertson, A. S.; Denton, R.; Grace, J. E.; Morrison, J.; Raybon, J.; Zhuo, X.; Snow, K.; Padmanabha, R.; Agler, M.; Esposito, K.; Harden, D.; Prack, M.; Varma, S.; Wong, V.; Zhu, Y.; Zvyaga, T.; Gerritz, S.; Marcini, L. R.; Higgins, M. A.; Shi, J.; Wei, C.; Cantone, J. L.; Drexler, D. M.; Macor, J. E.; Olson, R. E.; Ahljianian, M. K.; Albright, C. F. Identification and preclinical pharmacology of the γ -secretase modulator BMS-869780. *Int. J. Alzheimer's Dis.* **2014**, *2014*, 431858.
- (9) Gillman, K. W.; Starrett, J. E.; Parker, M. F.; Xie, K.; Bronson, J. J.; Marcini, L. R.; McElhone, K. E.; Bergstrom, C. P.; Mate, R. A.;

Williams, R.; Meredith, J. E.; Burton, C. R.; Barten, D. M.; Toyn, J. H.; Roberts, S. B.; Lentz, K. A.; Houston, J. G.; Zaczek, R.; Albright, C. F.; Decicco, C. P.; Macor, J.; Olson, R. E. Discovery and evaluation of BMS-708163, a potent, selective, and orally bioavailable γ -secretase inhibitor. *ACS Med. Chem. Lett.* **2010**, *1*, 120–124.

(10) Kimura, T.; Kawano, K.; Doi, E.; Kitazawa, N.; Takaishi, M.; Ito, K.; Kaneko, T.; Sasaki, T.; Miyagawa, T.; Hagiwara, H.; Yoshida, Y. Preparation of bicyclic cinnamides as amyloid-beta production inhibitors. U.S. Patent Application 2007/0117839 A1, 2007.

(11) Zhu, Z.; Greenlee, W. J.; Sun, Z.-Y.; Gallo, G.; Asberom, T.; Huang, X.; Zhu, X.; McBriar, M. D.; Pissarnitski, D. A.; Zhao, Z.; Xu, R.; Li, H.; Palani, A.; Mazzola, R. D., Jr.; Clader, J.; Josien, H.; Qin, J. Preparation of substituted alkenyloxadiazole derivatives and analogs as gamma-secretase modulators. WO 2008/137139 A1, 2008.

(12) For a review of GSM chemotypes, see Bursavich, M. G.; Harrison, B. A.; Blain, J.-F. Gamma secretase modulators: new Alzheimer's drugs on the horizon? *J. Med. Chem.* **2016**, *59*, 7389–7409.

(13) Oddo, S.; Caccamo, A.; Shepherd, J. D.; Murphy, M. P.; Golde, T. E.; Kaye, R.; Metherate, R.; Mattson, M. P.; Akbari, Y.; LaFerla, F. M. Triple-transgenic model of Alzheimer's disease with plaques and tangles: intracellular A β and synaptic dysfunction. *Neuron* **2003**, *39*, 409–421.

(14) The stability in liver microsomes was determined by a high-throughput assay using 3 μ M substrate concentration and 1 mg/mL microsomal protein. Incubations were performed at 37 °C in sodium phosphate buffer (100 mM), pH 7.4, and quenched after 10 min. Samples were analyzed by LC–MS/MS, and the remaining percentage of parent substrate was reported.

(15) Toyn, J. H.; Ahljanian, M. K. Interpreting Alzheimer's disease clinical trials in light of the effects on amyloid- β . *Alzheimer's Res. Ther.* **2014**, *6*, 14.

(16) Hughes, J. D.; Blagg, J.; Price, D. A.; Bailey, S.; DeCrescenzo, G. A.; Devraj, R. V.; Ellsworth, E.; Fobian, Y. M.; Gibbs, M. E.; Gilles, R. W.; Greene, N.; Huang, E.; Krieger-Burke, T.; Loesel, J.; Wager, T.; Whiteley, L.; Zhang, Y. Physicochemical drug properties associated with in vivo toxicological outcomes. *Bioorg. Med. Chem. Lett.* **2008**, *18*, 4872–4875.

(17) Wager, T. T.; Hou, X.; Verhoest, P. R.; Villalobos, A. Moving beyond rules: the development of a central nervous system multiparameter optimization (CNS MPO) approach to enable alignment of druglike properties. *ACS Chem. Neurosci.* **2010**, *1*, 435–449.

(18) Pettersson, M.; Stepan, A. F.; Kauffman, G. W.; Johnson, D. S. Novel γ -secretase modulators for the treatment of Alzheimer's disease: a review focusing on patents from 2010 to 2012. *Expert Opin. Ther. Pat.* **2013**, *23*, 1349–1366.

(19) Toyn, J. H.; Boy, K. M.; Raybon, J.; Meredith, J. E.; Robertson, A. S.; Guss, V.; Hoque, N.; Sweeney, F.; Zhuo, X.; Clarke, W.; Snow, K.; Denton, R. R.; Zuev, D.; Thompson, L. A.; Morrison, J.; Grace, J.; Berisha, F.; Furlong, M.; Wang, J.-S.; Lentz, K. A.; Padmanabha, R.; Cook, L.; Wei, C.; Drexler, D. M.; Macor, J. E.; Albright, C. F.; Gasior, M.; Olson, R. E.; Hong, Q.; Soares, H. D.; AbuTarif, M.; Ahljanian, M. K. Robust translation of γ -secretase modulator pharmacology across preclinical species and human subjects. *J. Pharmacol. Exp. Ther.* **2016**, *358*, 125–137.

(20) Nanosuspension d_{50} was 0.26 μ m; d_{90} was 0.44 μ m.

(21) See Dayneka, N. L.; Garg, V.; Jusko, W. J. Comparison of four basic models of indirect pharmacodynamic responses. *J. Pharmacokin. Biopharm.* **1993**, *21*, 457–478. and Sharma, A.; Jusko, W. J. Characterization of four basic models of indirect pharmacodynamic responses. *J. Pharmacokin. Biopharm.* **1996**, *24*, 611–635. as utilized in Albright, C. F.; Dockens, R. C.; Meredith, J. E.; Olson, R. E.; Slemmon, R.; Lentz, K. A.; Wang, J.-S.; Denton, R. R.; Pilcher, G.; Rhyne, P. W.; Raybon, J. J.; Barten, D. M.; Burton, C.; Toyn, J. H.; Sankaranarayanan, S.; Polson, C.; Guss, V.; White, R.; Simutis, F.; Sanderson, T.; Gillman, K. W.; Starrett, J. E.; Bronson, J.; Sverdlov, O.; Huang, S.-P.; Castaneda, L.; Feldman, H.; Coric, V.; Zaczek, R.; Macor, J. E.; Huston, J.; Berman, R. M.; Tong, G. Pharmacodynamics

of selective inhibition of gamma-secretase by avagacestat. *J. Pharmacol. Exp. Ther.* **2013**, *344*, 686–695.

(22) Assay and data analysis methodology principles used in this study were as described in Ghanbari, F.; Rowland-Yeo, K.; Bloomer, J. C.; Clarke, S. E.; Lennard, M. S.; Tucker, G. T.; Rostami-Hodjegan, A. A critical evaluation of the experimental design of studies of mechanism based enzyme inhibition, with implications for in vitro-in vivo extrapolation. *Curr. Drug Metab.* **2006**, *7*, 315–334.

(23) $1000\lambda < 10$ indicates minor drug–drug interactions. See Mayhew, B. S.; Jones, D. R.; Hall, S. D. An in vitro model for predicting in vivo inhibition of cytochrome P450 3A4 by metabolic intermediate complex formation. *Drug Metab. Dispos.* **2000**, *28*, 1031–1037.

(24) Aronov, A. M. Common pharmacophores for uncharged human ether-a-go-go-related gene (hERG) blockers. *J. Med. Chem.* **2006**, *49*, 6917–6921.

(25) Hagemann, H. Synthesis and reactions of *N*-chlorocarbonyl isocyanate. *Angew. Chem., Int. Ed. Engl.* **1977**, *16*, 743–750.

(26) Strotman, N. A.; Ramirez, A.; Simmons, E. M.; Soltani, O.; Parsons, A. T.; Fan, Y.; Sawyer, J. R.; Rosner, T.; Janey, J. M.; Tran, K.; Li, J.; LaCruz, T. E.; Pathirana, C.; Ng, A. T.; Deerberg, J. Enantioselective synthesis of a γ -secretase modulator via vinylogous dynamic kinetic resolution. *J. Org. Chem.* **2018**, *83*, 11133.

(27) Soares, H. D.; Gasior, M.; Toyn, J. H.; Wang, J.-S.; Hong, Q.; Berisha, F.; Furlong, M. T.; Raybon, J.; Lentz, K. A.; Sweeney, F.; Zheng, N.; Akinsanya, B.; Berman, R. M.; Thompson, L. A.; Olson, R. E.; Morrison, J.; Drexler, D. M.; Macor, J. E.; Albright, C. F.; Ahljanian, M. K.; AbuTarif, M. The γ -secretase modulator, BMS-932481, modulates A β peptides in the plasma and cerebrospinal fluid of healthy volunteers. *J. Pharmacol. Exp. Ther.* **2016**, *358*, 138–150.

(28) Additional related information may be found in Boy, K. M.; Guernon, J. M.; Macor, J. E.; Olson, R. E.; Shi, J.; Thompson, L. A.; Wu, Y.-J.; Xu, L.; Zhang, Y.; Zuev, D. S. Compounds for the reduction of beta-amyloid production. U.S. Patent 8,486,952, July 16, 2013.